

THE HISTORY OF TIDAL DISRUPTION EVENTS IN GALACTIC NUCLEI

DANOR AHARON, ALESSANDRA MASTROBUONO BATTISTI & HAGAI B. PERETS
Physics Department, Technion - Israel Institute of Technology, Haifa, Israel 3200003
Draft version June 24, 2021

Abstract

The tidal disruption of a star by a massive black hole (MBH) is thought to produce a transient luminous event. Such tidal disruption events (TDEs) may play an important role in the detection and characterization of MBHs and probe the properties and dynamics of their nuclear stellar clusters (NSCs) hosts. Previous studies estimated the recent rates of TDEs in the local universe. However, the long-term evolution of the rates throughout the history of the universe has been hardly explored. Here we consider the TDE history, using evolutionary models for the evolution of galactic nuclei. We use a 1D Fokker-Planck approach to explore the evolution of MBH-hosting NSCs, and obtain the disruption rates of stars during their evolution. We complement these with an analysis of TDEs history based on N-body simulation data, and find them to be comparable. We consider NSCs that are built-up from close-in star-formation (SF) or from SF/clusters-dispersal far-out, a few pc from the MBH. We also explore cases where primordial NSCs exist and later evolve through additional star-formation/cluster-dispersal processes. We study the dependence of the TDE history on the type of galaxy, as well as the dependence on the MBH mass. These provide several scenarios, with a continuous increase of the TDE rates over time for cases of far-out SF and a more complex behavior for the close-in SF cases. Finally, we integrate the TDE histories of the various scenarios to provide a total TDE history of the universe, which can be potentially probed with future large surveys (e.g. LSST).

1. INTRODUCTION

A tidal disruption event (TDE) by a massive black hole (MBH) occurs when a star comes closer than its tidal radius (approximately given by $r_t = (M_\bullet/m_\star)^{1/3}r_\star$; where M_\bullet is the mass of the MBH, m_\star is the mass of the star and r_\star is its radius). The star is then pulled apart by the tidal forces by the MBH, part of its material is ejected away and part is accreted on the MBH (e.g. Rees 1988). The explosive disruption itself, and the later accretion on the MBH likely give rise to transient energetic phenomena potentially observable (with more than ten potential detections to date) with current and future telescopes (e.g. Gezari 2014).

MBHs are thought to exist in a significant fraction of all galactic nuclei. Due to their high mass ($10^5 - 10^9 M_\odot$), they dominate the gravitational potential in the nuclear star clusters (NSCs) which typically host them (at least at the $10^5 - 10^8 M_\odot$ MBH mass regime); the orbits of stars in the central parsecs around MBHs are therefore governed by the potential of the MBHs. The long-term dynamical evolution of the stars in the region of influence of the MBH is also determined by their interactions and mutual gravitational scatterings with other stars in the NSC. These can be modeled using a Fokker-Planck (FP) approach to describe the diffusive behavior of stars in NSC. (Bahcall and Wolf 1976), where the close approaches of stars to the MBH leading to their tidal disruption can be modeled as a sink-term in the FP equations. TDE rates calculated following such an approach typically give rise to rates of the order of 10^{-5} up to 10^{-3}yr^{-1} per galaxy in the local Universe, assuming some steady state condition of the NSC (e.g. Wang and Merritt 2004, and references therein).

Since the 1980's tidal disruption of stars by MBHs were suggested to occur in galactic nuclei and produce

luminous transient events with unique signatures (Rees 1988). The signatures can teach us both on the dynamics in galactic nuclei as well as on the conditions very close to MBHs, and their properties. Such TDEs have since been extensively studied theoretically, and a significant observational effort has been put in their detection (Gezari 2014). Many studies have estimated the rates of TDEs (e.g. Magorrian and Tremaine 1999, Merritt (2009) and Brockamp et al. 2011) in the local universe, and several estimates have been derived based on direct observations of TDE-candidates in recent years (Khabibullin and Sazonov 2014; van Velzen and Farrar 2014). Since the structure and the properties of NSCs vary with time, it is expected that the TDE rates will change accordingly. Moreover, the change of TDE rates can be used as a proxy for characterizing the properties of NSCs and/or the history of the build-up of MBHs and NSCs in the universe. In particular, future deep surveys may allow the detection of TDEs from earlier stages of cosmological evolution arising from younger galaxies, and potentially provide a handle on the TDE history (Gezari 2014). Nevertheless, the evolution of TDE rates with time and their dependence on the NSC and star-formation history and evolution have been little studied.

In this work, we explore the TDEs history (TDH) by studying the rate of tidal disruption of stars in NSCs. We simulate the evolution of NSCs in several types of galaxies by FP analysis as well as N-body simulations. We obtain the TDE rates as a function of their evolutionary history, and find that they are affected by the NSC structure and its build-up history. By integrating the TDE rates from galaxies of each type we obtain the total galaxy averaged TDH of the universe expected to be observed. We thereby provide a first global estimate of the TDH accounting for NSC build-up, albeit with simple models.

In the following we begin by a brief description of the Fokker-Planck analysis and N-body simulations of evolving clusters. We describe our approach of evaluating a sink term from FP analysis for calculating the tidal disruption rate. We then present the TDH and its dependence on the MBH mass and the NSC build-up history in different types of galaxies. Finally, we consider the global, galaxy averaged, TDH of the universe evaluated by integrating the TDE rates arising from the different types of galaxies (and their correspondent evolutionary histories) and relevant MBH masses. We note, that our model is based on typical NSCs that undergo basic processes and their dynamics are dominated by two-body relaxation. The model can be expanded, and future works may include other processes and properties in NSC such as non uniform stellar mass, self-consistent potential, non-spherical NSCs etc. Here we provide a first study of the history of TDEs using simple models.

2. METHODS

In our work we explore the tidal disruption rates in NSCs through their evolution in time. We focus on simple, spherical NSCs that evolve through in-situ star formation (SF) (Aharon and Perets 2015), and study other cases of NSCs that are built-up through consecutive infalls of massive clusters or evolve from a pre-existing stellar cusp. The main analysis method used in our work is based on the numerical solution of the FP equation, complemented by N-body simulations of NSCs evolution.

Our model includes a stellar cluster, the NSC, harboring a central MBH. It focuses on the stars in the central few parsecs of the NSC, and in particular in the range between the tidal radius - $r_t \approx r_*(M_\bullet/M_*)^{1/3}$ below which regular stars are disrupted by the MBH, and the radius of influence where the stellar motions are dominated by the MBH potential, defined by

$$r_h = GM_\bullet/\sigma_\star^2, \quad (1)$$

where r_* , and M_* are the typical radius and mass of stars in the NSC, respectively; and σ_\star is the velocity dispersion of stars just outside the NSC. For $r > r_h$ the original model following Bahcall and Wolf (1976, hereafter BW) assumes the existence of a “thermal bath” which supplies stars to the inner region of the galactic nucleus. The stellar orbits within r_h are assumed to be Keplerian in this range. The relaxation time, that dominates the timescale of the stellar cluster, is defined as

$$T_r \approx \frac{\sigma^3}{G^2 M_\star \rho \ln(\Lambda)} \quad (2)$$

Where ρ is the stellar density, and $\ln(\Lambda)$ is the Coulomb logarithm, a factor which is related to the scale of the system ($\ln(\Lambda) \approx 10$).

2.1. Fokker-Planck analysis and N-body simulation

The FP model, extensively used in our work, consists of a time and energy-dependent, angular momentum-averaged particle conservation equation. It has the form:

$$\frac{\partial f(E, t)}{\partial t} = -AE^{-\frac{5}{2}} \frac{\partial F}{\partial E} - F_{LC}(E, T) + F_{SF}(E, T) \quad (3)$$

where

$$A = \frac{32\pi^2}{3} G^2 M_\star^2 \ln(\Lambda) \quad (4)$$

The term $F = F[f(E), E]$ is related to the stellar flow, and plays an important role in the evolution of the stellar cluster. It presents the flow of stars in energy space due to two-body relaxation, it is defined by:

$$F = \int dE' \left(f(E, t) \frac{\partial f(E', t)}{\partial E'} - f(E', t) \frac{\partial f(E, t)}{\partial E} \right) (\max(E, E'))^{-\frac{3}{2}} \quad (5)$$

The addition of the source term that represents the SF has the form:

$$F_{SF}(E, T) = \frac{\partial}{\partial t} (\Pi(E) E_0 E^\alpha) \quad (6)$$

$\Pi(E)$ is a rectangular function, which boundaries correspond to the region where new stars are assumed to form; E_0 is the source term amplitude; and F_{SF} is a power-law function with a slope α , defining the SF distribution in phase space. For a detailed description of the Fokker-Planck analysis see Aharon and Perets (2015) where the same analysis was used for studying the evolution of NSCs with in-situ SF. Note that the sink term $F_{LC}(E, T)$ in Eq. 3 is used for evaluating the tidal disruption rates in our models. This term represents stars with energies in the interval $(E, E + dE)$ that flow into the MBH (mostly due to angular momentum change; the sink-term represent the effective loss in energy space; see Bahcall and Wolf 1977; Lightman and Shapiro 1977), and are therefore lost from the system (see Merritt 2013a for detailed overview of loss cone analysis).

For modeling tidal disruption through N-body simulations, we follow the same methods and similar assumptions, as well as make the same use of the same code in Perets and Mastrobuono-Battisti (2014) and Mastrobuono-Battisti et al. (2014), where the TDE rates are evaluated. For a detailed method explanation along with the initial conditions of the infalling clusters and TDEs estimation, see Mastrobuono-Battisti et al. (2014). In brief, we run direct N-body simulations (using the ϕ GRAPE code, Harfst et al. 2007) of the consecutive infall and merging of a set of 12 single-mass globular clusters each with mass of $10^6 M_\odot$, inspiralling from a galactocentric distance of 20pc.

3. MODELS

3.1. Formation and evolution of NSCs

In our study, we explore the TDH through two formation/evolutionary models of NSCs: in-situ star formation and cluster infall. The study is done by using the FP analysis to simulate an evolving NSC with an addition of extra source term (see Aharon and Perets 2015 for the full analysis). In the in-situ SF model we consider two possible cases: NSCs that are entirely built-up from the in-situ SF, and NSCs that evolve from an initial steady state BW distribution (hereinafter “built-up SF” origin and “primordial cusp origin”, respectively). In both of the scenarios, the initial density profile is determined from an arbitrary initial distribution function (DF). For the bound stars inside the radius of influence in the primordial cusp scenario the DF takes the form of

$f(E, t_0) \propto E^{0.25}$ (corresponding to the BW steady-state cusp which has the form of $n \propto r^{-7/4}$). The normalization of the number density at the radius of influence for each scenario is given in table 3.1. We consider different masses for the hosted MBH in their centers, where the density profiles of the NSCs are normalized in the same way as done in Wang and Merritt (2004), where the parameters were taken from typical galaxies (e.g. NGC 4551/4621). The velocity dispersion (which is taken into account in the calculation of the radius of influence) is evaluated from the M-Sigma relation: $M_{\bullet} \propto \sigma^{4.36}$, (Merritt and Ferrarese 2001).

MBH mass [M_{\odot}]	5×10^5	1×10^6	5×10^6	1×10^7
density profile at r_h [pc^{-3}]	6×10^3	1×10^4	4×10^4	1×10^5

TABLE 1
DENSITY PROFILE AT r_h OF NSCs FOR DIFFERENT MBH MASSES

In the built-up SF scenario the initial DF is evaluated according to the term F_{SF} (Eq. 6), where the initial number density is equal to the added number density every time step. For both of the scenarios, The chosen slope of the SF function is motivated by the observed power-law (Do et al. 2009; Bartko et al. 2009) distribution of young stars observed in the young stellar disk in the GC. The DF of the unbound stars ($-\infty < r < r_h$) has the form of a Maxwellian distribution. We study the TDE rates throughout the evolution of NSCs and For each scenario we tested several types of SF history corresponding to the galaxy type studied (see Section 3.2). Though we use the FP approach for our modeling of the TDH, we also complement our analysis with N-body simulations of the cluster-infall scenario. As discussed later on, we find that models of in-situ SF in the outer regions of an NSC evolve very similarly to those of cluster infall, since the clusters shed their material in the same regions, effectively providing a source term similar to that arising from SF. Therefore our models of in-situ SF in the outer regions of an NSC effectively well capture models of cluster-infall, at least in terms of the TDE rates under the assumptions made in our study.

3.2. Star formation history in different type of galaxies

We followed the evolution of several types of galaxies with different SF scenarios. For each type of galaxy and SF scenario we evaluated the TDE rates and their evolution. We considered the following simplified cases: (1) An elliptical galaxy with SF occurring only at the early stages of the evolution of the NSC; and (2) spiral galaxy with either continuous SF or repeating bursts of SF occurring throughout the evolution of the NSC to present days. The correspondence between galaxy type and its typical SF history follows Madau and Dickinson (2014). We used a simplified model to describe the non-continuous SF star-burst scenario, where we assume the bursts occur at equally spaced time intervals (Gyr), at ten times the rate of the continuous SF models, but only for 100 Myrs (as to have the same total SF averaged rate). We summarize the types of galaxies and the SF scenarios simulated in our work in Table 2. Note, that we also study different scenarios for the regions where SF may occur; either in the range between 2.0 – 3.5pc

or in the range 0.05 – 0.1pc from the MBH. The ranges that were chosen for SF in our work are motivated by the observed existence of a possibly star-forming circumnuclear gaseous disk in the range of 2-5pc in the Galactic center (similar young stellar populations are observed in other galactic nuclei, e.g. Seth et al. 2006). Most of the presented SF scenarios are based on these observations. The close-in SF region ($< 0.1\text{pc}$) is motivated by the existence of a nuclear stellar disk of young stars very close to the MBH in the Galactic center (e.g. Do et al. 2009; Bartko et al. 2009). The averaged rates of SF were set to $10^{-4} - 5 \times 10^{-3} \text{yr}^{-1}$, motivated by the observed number of stars in the central parsecs of galactic nuclei, as to obtain a total mass of $\sim 10^6 - 5 \times 10^7 M_{\odot}$ comparable to the masses of NSCs derived from observations of the GC and extragalactic NSCs (Seth et al. 2006).

In addition, we note that the range of 2.0 – 3.5pc is also representative of the range where a disrupted cluster dispenses its stars close to the MBH, thereby building-up the NSC stellar population (e.g. Antonini et al. 2012; Perets and Mastrobuono-Battisti 2014; the exact cluster tidal radius depends on the MBH and NSC mass and could have a slightly larger range). Finally, we also considered different rates of SF in the NSC to access their overall effects on the TDH. All models used are summarized in Table 1. Note that bursting SF models where SF occurs in the outer regions also serve as good proxies for the cluster infall model, as we discuss later on.

We simulated the evolution of each NSC (described in Table 2) with its corresponding TDE for four different masses of MBHs: $5 \times 10^5 M_{\odot}$, $1 \times 10^6 M_{\odot}$, $5 \times 10^6 M_{\odot}$ and $1 \times 10^7 M_{\odot}$ in order to evaluate a general form of TDEs dependency on MBH mass. For each studied mass of MBH the appropriate relaxation time corresponding to the velocity dispersion (evaluated from M-Sigma relation, Merritt and Ferrarese 2001) was determined, and used to produce the primordial clusters considered in the relevant models. The rates of tidal disruptions were then evaluated throughout the NSC evolution. The evolution of NSCs hosting MBHs of higher masses is not discussed in this work, since the tidal radius for MS stars falls below the Schwarzschild radius ($2GM_{\bullet}/c^2$). Therefore, MBH with higher masses would not contribute to the TDE rates of typical main-sequence stars. Lower mass MBHs may also exist, though there is little observational evidence for their current existence, but this is likely due to current observational limitations. Nevertheless, such low mass MBHs may give rise to TDEs with significantly different observational signatures, and we therefore limit our study only to more massive MBHs.

3.3. Assumptions and Limitations

The disruption rates of stars by MBHs depend both on the NSC properties as well as on several possible physical processes. These processes include for example the presence of massive perturbers, that refill the loss cone (e.g. Perets et al. 2007), the evolution of central MBHs binaries and the effects of non spherically symmetric potentials in the nucleus (see Merritt 2013b for a comprehensive review). Some of these processes are efficient in increasing the TDE rates, but typically operate only on short timescales (e.g. binary MBH mergers), while the level of non-sphericity of galactic nuclei is not well

Model (Galaxy type)	SF rate (yr^{-1})	Spatial regions of SF (pc)	Epoch of SF	NSC Origin
E (elliptical)	5×10^{-3}	2.0 – 3.5; 0.05 – 0.1	0-1 Gyr	Primordial BW cusp
			0-1 Gyr	build-up
	10^{-3}	2.0 – 3.5	0-1 Gyr	Primordial BW cusp
			0-1 Gyr	build-up
S_0 (spiral with continuous SF)	5×10^{-4}	2.0 – 3.5; 0.05 – 0.1	0-10 Gyr	Primordial BW cusp
			0-10 Gyr	build-up
S_B (spiral with bursts of SF)	Bursts of 5×10^{-3}	2.0 – 3.5; 0.05 – 0.1	bursts of 100 Myr every 1 Gyr	Primordial BW cusp
				build-up
	Bursts of 10^{-3}	2.0 – 3.5		Primordial BW cusp
				build-up

TABLE 2
MODELS FOR NUCLEAR STELLAR CLUSTERS AND STAR FORMATION IN DIFFERENT TYPES OF GALAXIES.

known. Our model focuses the TDEs for number of SF scenarios including different rates and different ranges. A similar TDE history model was suggested by Merritt (2009) whose work was based on different evolution scenarios of NSCs which does not include SF. A comparison between Merritt’s work and this study results is discussed in section 4.1.1.

Another important assumption is that the MBHs in our models evolve and change their mass. This change is done by adding the mass of the disrupted stars to the MBH during the evolution of an NSC. We emphasize, however, that the growth of the MBH mainly affects the TDE rates in the lower rates of SF scenarios and for initial low masses of MBH, in which cases the total added mass becomes comparable to the initial mass of the MBH. In these cases, the TDE rates decline with time (see Fig. 5), while the TDE rates grow with time for the more massive MBHs.

We continuously change the NSC structure up to the radius of influence according to the evolution of the FP models. As the mass of the MBH grows we change the velocity dispersion σ_* assuming the $M-\sigma$ relation holds at any given time. The radius of influence (Eq. 1) is then changed according to the updated mass and velocity dispersion, and the outer boundary condition of the thermal bath also change accordingly, following Wang and Merritt (2004). We note and caution that this is not a trivial assumption; its advantage is in consistently relating the MBH, the velocity dispersion and the stellar density outside the NSC, and therefore, by definition producing a final NSC and environmental configuration which is in accordance with the observed $M-\sigma$ relation today (though the relation is defined in the context of the velocity dispersion at larger radii). The disadvantage is in using an ad-hoc assumption in which the $M-\sigma$ relation is continuously kept at all times; whether this holds is currently unknown. To the best of our knowledge previous studies used either a constant outer boundary conditions (e.g. Bahcall and Wolf 1976, 1977; Cohn and Kulsrud 1978), or had self-consistently evolving open outer boundaries (Murphy et al. 1991); in this latter case the initial conditions determined the velocity dispersion and the density in the NSC outer region. Since no additional boundary conditions or an outer thermal bath were introduced, the conditions in the outer regions (where relaxation is slow) hardly changed (see below),

and the NSCs was effectively described as isolated system, unrelated to the larger scale evolution of the galaxy. Thereby it could not reproduce a configuration based on the $M-\sigma$ relation today, unless arbitrarily put by hand as initial conditions. Given these limitations and the debated understanding of MBH feedback and the origin of the $M-\sigma$ relation, we believe the ad-hoc assumption we use is quite reasonable, and compared with other choices it introduces a plausible relation between the NSC and the larger scale environment consistent with current observations.

Our modeling accounts for the NSC stellar population (the density profile) up to the radius of influence in the evolving NSC, while the stellar population outside the region is assumed to be consistent with the large scale galactic bulge, as described above. We assume the potential is dominated by the MBH and neglect the contribution from the stellar population of the NSC, i.e. the contribution of the stellar component up to the radius of influence is neglected, similar to the original BW study. Up to the radius of influence this simplifying assumption is justified, while far from the MBH it breaks down. Nevertheless, at these regions the relaxation time becomes larger than the Hubble time, and the background does not change due to the NSC internal evolution. The intermediate regions beyond the radius of influence, in which relaxation time can still be significantly shorter than a Hubble time are small, and therefore our simplified modeling should still well capture the overall dynamics of the NSC.

For our final integrated TDH results (see Section 4.3), we extended the range of MBHs masses between 10^5 and $5 \times 10^7 M_\odot$ by using the interpolated power-law function that describes the dependence between TDE rates and MBH mass (Eq. 7). We do not consider TDEs from lower mass MBHs, or TDEs of evolved stars, which could be relevant even for MBHs above this mass range.

Here we only consider simple models of spherical NSCs hosting non-evolving MBHs of given masses with relaxation dominated by two-body scattering of low mass (Sun-like) stars. Other models are beyond the scope of this initial study and will be explored elsewhere.

4. RESULTS & DISCUSSIONS

4.1. Tidal disruption events history from Fokker-Planck analysis

4.1.1. Cluster infall and star-formation in NSC outskirts

Stellar clusters infalling into the nuclear regions are typically disrupted and shed their stars at scales of a few pc from the Galactic center, due to their disruption by the potential of the MBH and the existing NSC (e.g. Perets and Mastrobuono-Battisti 2014). There is also evidence for star-formation, young stellar populations and dense star-forming clumps in these regions (e.g. the nuclear stellar disk in the Galactic center, and young stellar populations in many galactic nuclei, Seth et al. 2006; Oka et al. 2011). Together, these suggest that both in-situ SF and cluster infall scenarios give rise to a source term of stars in regions at a few pc from the MBH. In the following we present the results of FP calculations, where star-formation/cluster infall scenarios are assumed to introduce new stars, a “source term” in the FP models, in the regions between 2-3.5 pc. Note that we use the term SF throughout the following discussion, but it effectively also represents a source term of stars from infalling clusters.

As discussed in the previous sections, we have explored the TDE rates as a function of the SF rate and characteristics. Figures 1 and 2 show the evolution of the TDE rates with time for various models of the NSCs. As expected, the TDE rates grow with time as the NSC stellar population and the density of the NSCs increase due to star-formation. The early times TDE rates in the models of early star-formation (ellipticals) are significantly higher than the corresponding rates in the models with long term SF (spirals). However, at later times the NSCs in both cases saturate to similar levels as the NSCs reach similar densities at late times (in cases of the same total cumulative SF throughout the evolution). The TDE rates in NSCs with initial primordial cusps are generally higher, since the overall stellar populations are larger. The rise in the TDE rates is not linear as in the built-up NSCs models as relaxation processes are more pronounced already at early stages. Since typical relaxation times are longer than the length of SF bursts in our models, it is not surprising that the SF bursts models behave very similarly to those with continuous SF (with same averaged SF rates). Henceforth we omit the results for SF burst models, which are essentially the same as those in the continuous SF models.

The high SF during the first Gyr in the elliptical galaxies models give rise to a significant increase of the stellar population in the NSC, and correspondingly leads to shorter relaxation times, and higher densities. In turn the TDE rates rapidly increase during this epoch, due to these effects, and the increase becomes shallower only at later times after the end of the SF epoch. Nevertheless, the rates continue to grow in time even after 10 Gyr of evolution as stars from the galaxy slowly diffuse into the NSC. In the spiral galaxy models SF is continuous throughout the evolution, and the TDE rates similarly increase in a more continuous manner.

In addition to the comparison between TDEs in different types of galaxies, we compare the TDE rates for different masses of MBHs ($5 \times 10^5 M_\odot$, $1 \times 10^6 M_\odot$, $5 \times 10^6 M_\odot$ and $1 \times 10^7 M_\odot$). We present the behavior of each scenario and for each of the MBH masses along with the evolution of the total mass of the NSC; see Figures 3 and 4. These probe the dependence of the TDE rates

on the mass of the MBHs. It can be clearly seen that the TDE rates decrease with the mass of the MBH. This result has already been discussed by Wang and Merritt (2004), and can be well understood from loss cone analysis (see Merritt 2013a).

Merritt (2009) have discussed the evolution of TDE rates with time in the case of a non-SF NSC. Though our models always include SF, the evolution of models of pre-existing NSCs in which only an early SF epoch occurs, evolve very similarly to the models explored in Merritt (2009), after the end of the SF. Such models generally predict a global decrease of TDE rates over time. A different trend exists in the evolution of TDE rates in models with long-term SF, in which the TDE rates slowly increase with time as the NSC keeps growing due to SF.

Fig. 5 shows the TDE rates for the models with lower SF rates and low MBH masses. Note that in the models with MBHs masses of $5 \times 10^5 M_\odot$ and $10^6 M_\odot$ the TDE rates decay with time. In these cases the restive increase in the MBH mass significantly increase the relaxation time leading to lower TDE rates, even though the total masses of the NSCs increase.

4.1.2. Star-formation in the inner regions of NSCs

In addition to the TDH presented above, corresponding to SF at a distance of 2 – 3.5pc, we also studied the TDH in a different scenario, where SF is assumed to mainly occur in the inner regions of NSCs. Evidence for such more nucleated SF can be found in our own galaxy, where a young stellar population is observed in the inner ~ 0.1 pc near the MBH; though it is not clear if such SF is typical (such regions can not yet be resolved in other galaxies), we consider this possibility for completeness. We followed the same conditions used in the previous scenarios, but we changed the range of SF to correspond to distances of 0.05 – 0.1pc. Figure 6 presents the TDEs history for SF rate of $5 \times 10^{-3} \text{yr}^{-1}$ and $5 \times 10^{-4} \text{yr}^{-1}$ for elliptical and spiral galaxies, respectively. On the right panel we notice a different behavior of the TDH for elliptical galaxy compared with the outskirt SF scenarios: while there is a rapid growth in the disruption rates during the epoch of SF, the rates decreases with time once the SF process is quenched. Since the stellar densities increase on relatively short times as many stars are formed close to the MBH, the NSC is initially far from its steady state configuration. The inner regions are “over-populated” and relaxation processes take time to redistribute these stars throughout the NSC. Since stars in these regions are more susceptible to being tidally disrupted (larger loss cone), the TDE rates increase rapidly, before the NSC structure re-equilibrates. The long-term SF occurring in spiral galaxies allows for relaxation processes to redistribute the stars, and the TDE rates increase more slowly, as the NSC is built-up.

4.1.3. Global SF in NSCs

In addition to the TDHs of NSCs evolving through an early SF epoch or through continuous SF (described in Table 2), we also studied models in which the SF follows the global universal SF history (i.e. Madau and Dickinson 2014) in such global models early SF is more significant, and then it gradually decrease by an order of of magnitude (Madau and Dickinson 2014). Such models are therefore expected to be more similar to

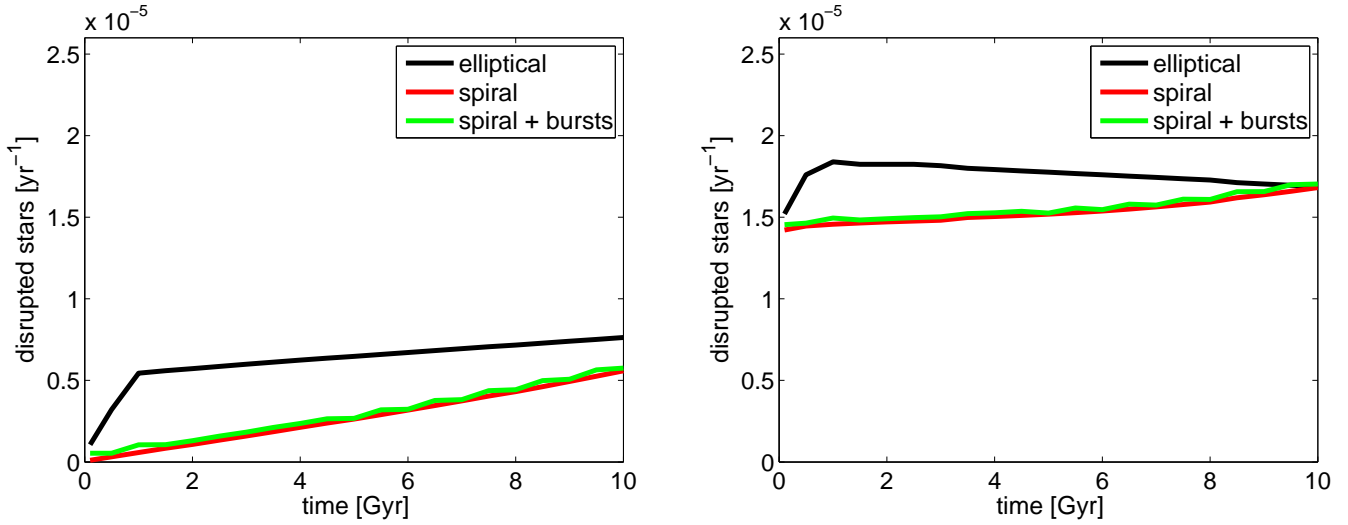


FIG. 1.— The evolution of TDEs for NSCs with an MBH of $4 \times 10^6 M_{\odot}$ for 3 types of galaxies, that are evolved through in-situ SF (left) and from a primordial cusp (right). The rates of SF are 10^{-3} and 10^{-4} stars \times year $^{-1}$ for elliptical and spiral galaxies respectively. The total number of stars formed throughout the evolution is the same; NSC with primordial cusps have a larger number of stars as they have similar SF histories but they also include the stellar populations of the primordial cusps.

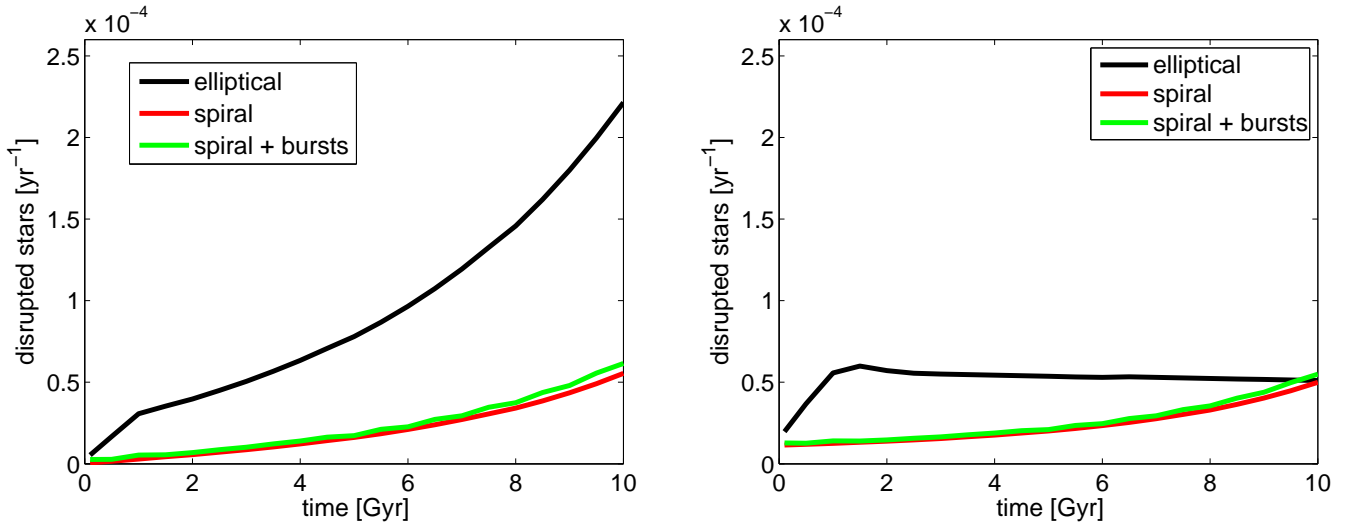


FIG. 2.— The TDH as shown in Figure 1 for higher rates of SF (5×10^{-3} and 5×10^{-4} stars \times year $^{-1}$ for elliptical and spiral galaxies respectively).

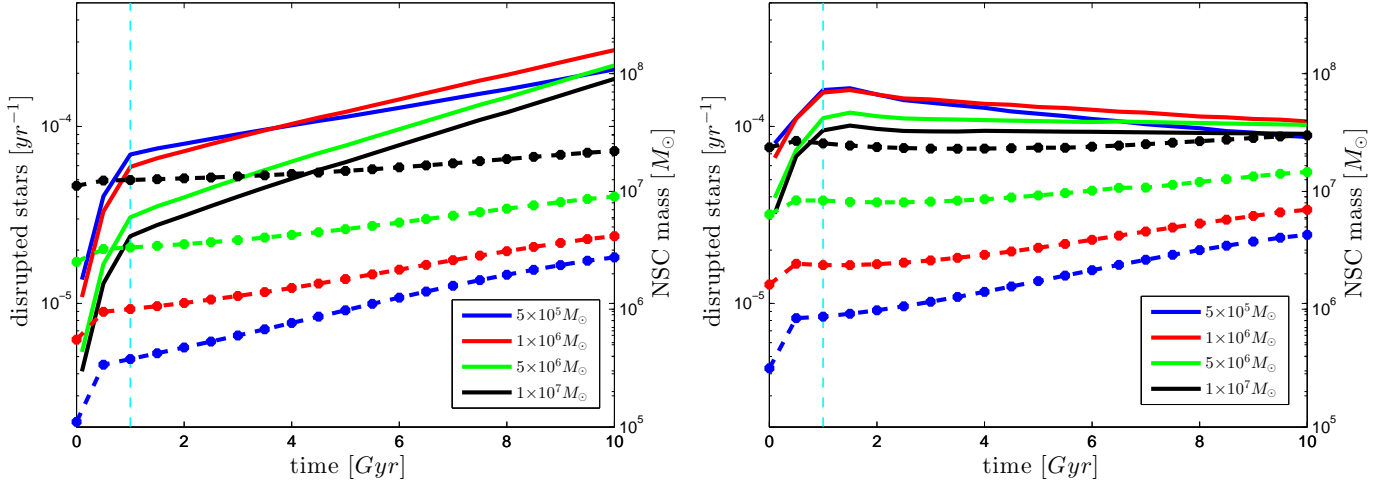


FIG. 3.— Evolution of TDE rates (continuous lines) for four different masses of MBHs for model E along with mass of the NSC (dashed lines). The cyan vertical dashed line marks the epoch at which the SF stops. NSC masses and the corresponding TDE rates of the same models are marked with the same colors. Left: TDH for NSC evolved from built-up star formation. Right: TDH for NSC evolved from a primordial cusp.

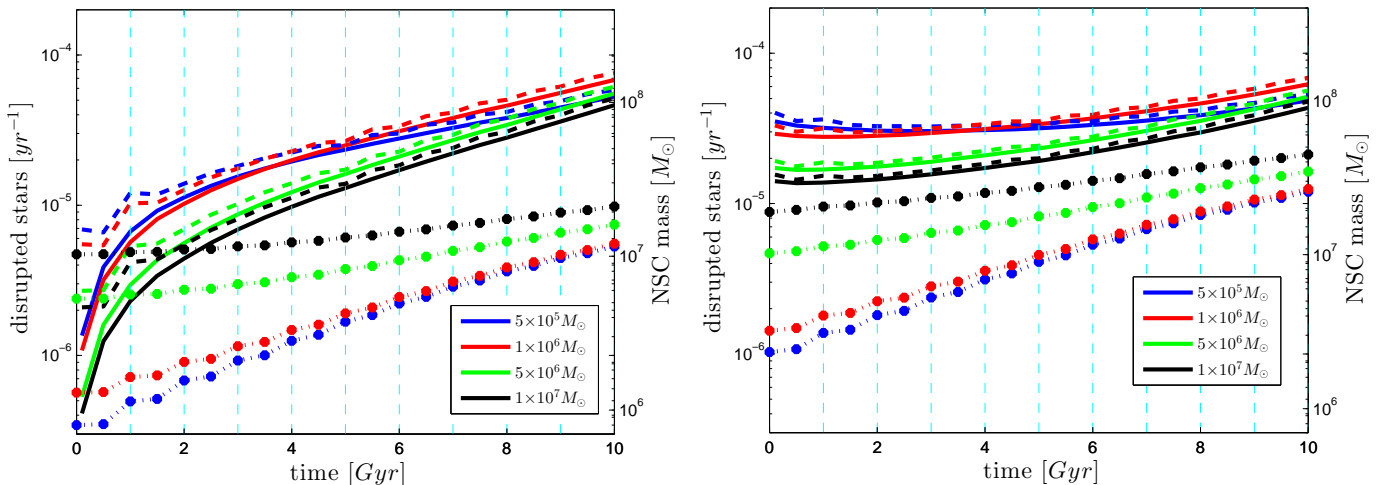


FIG. 4.— Evolution of TDE (continuous lines) rates for four different masses of MBHs for models S_0 (solid lines) and S_B (dashed lines). NSC masses and the corresponding TDE rates of the same models are marked with the same colors. The blue dashed lines mark the time of the SF bursts (every 1 Gyr). Left: TDH for NSC evolved from built-up star formation. Right: TDH for NSC evolved from a primordial cusp.

the early SF epoch models (“elliptical galaxies”). In Fig. 7 we show the results from three models, which confirm these expectations; these models show similar trends as those in Fig. 7.

4.2. Tidal disruption events history using N -body simulation data

Following the cluster infall study (described in Perets and Mastrobuono-Battisti 2014), we evaluated the disruption rates of stars based on data obtained from N -body simulations. This provides us with a complementary approach to the FP calculations, through a different type of analysis. As we show in the following the FP calculation for models with SF in the NSC outskirts and the calculations based on N -body data are generally comparable. Note that the N -body calculations are computationally expensive, and therefore we show only a single case, while our general main results (shown in

the previous sections) are based on the FP calculations. Note that direct calculation of the TDE rates from an N -body simulation requires appropriate resolution, number of particles and calibration. We have followed a more simplified approach where the N -body simulations only provide us with the effective radial density profile at any given point in time, from which we then calculate the TDE rate semi-analytically, similar to the approach used in Mastrobuono-Battisti, Perets & Loeb (2014). This avoids the obstacles arising from the direct calculations of TDE rates in N -body simulations, at the cost of a less accurate result, and the use of the simplifying assumption of an isotropic distribution.

In the cluster-infall scenario clusters are added to the system on equally spaced time intervals. They then inspiral and disrupt, and their stars build-up the NSC. To a large extent this is captured by the FP models which introduce stars in the NSC outskirts; since the infalling

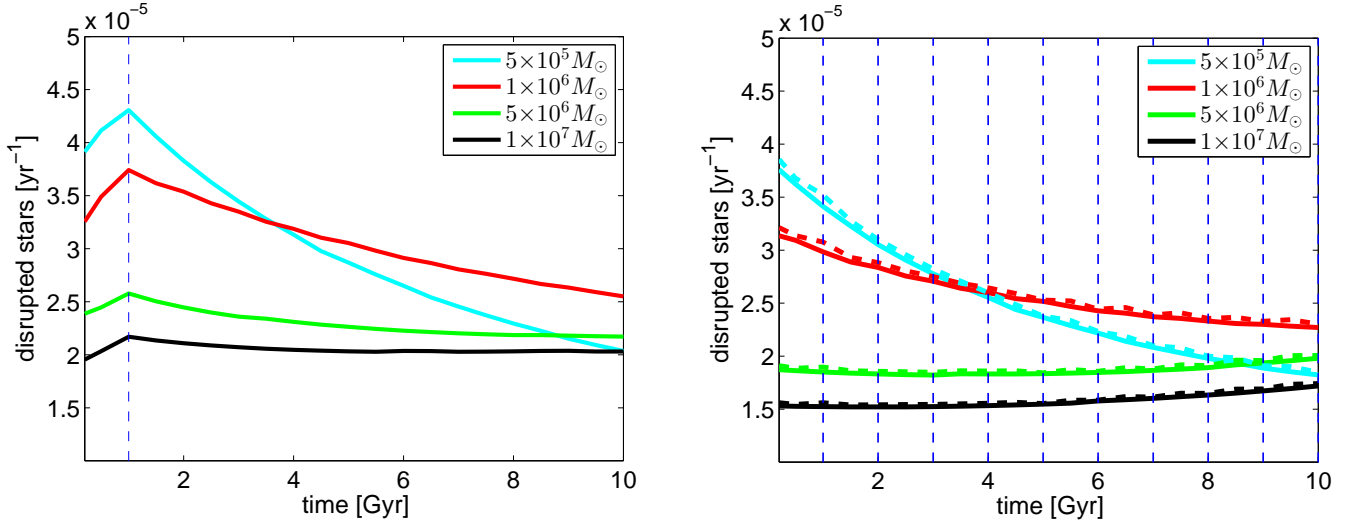


FIG. 5.— Evolution of TDE (continuous lines) rates for four different masses of MBHs for models E (left panel) and $S_0 S_B$ (right panel) for lower rates of SF. The dashed blue lines mark the epoch at which SF stops and the bursts of SF for E and S models respectively.

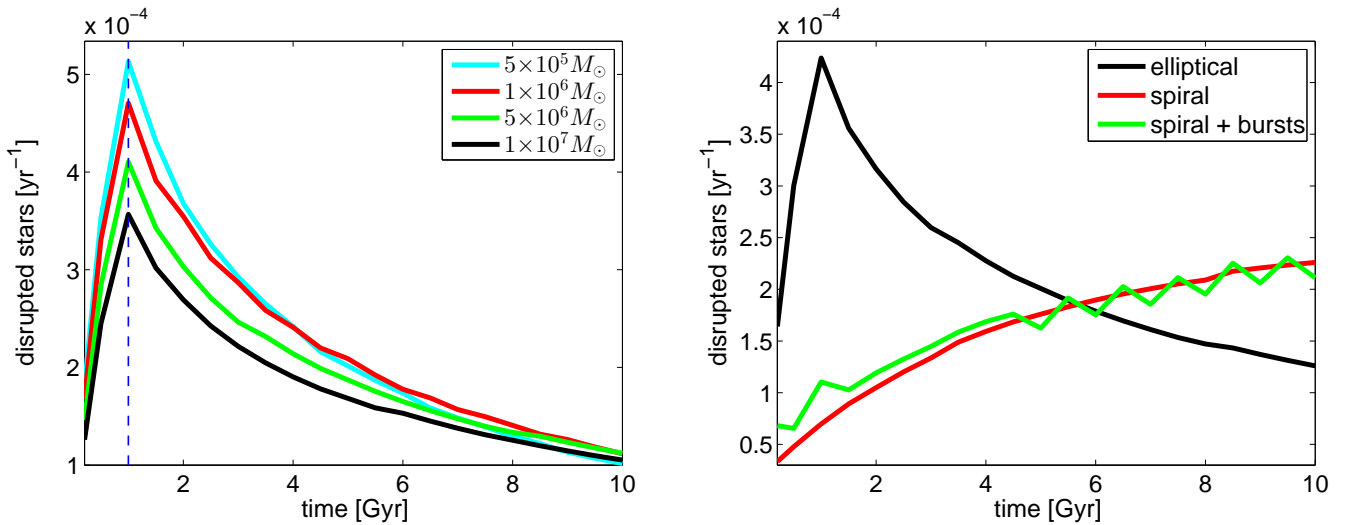


FIG. 6.— TDEs history for scenarios in which SF that takes place in the inner parsec (0.05-0.1pc), for NSCs that are built up through in-situ SF. Left: TDH evaluated for elliptical galaxies (SF occurs only in the first Gyr) for four masses of MBH. Right: TDE histories for three different types of galaxies for high SF rates ($5 \times 10^{-3} M_\odot$, similar to Figure 2)

clusters disperse in the same distance scales (few pcs), they introduce stars in the same manner as assumed in these FP models. We therefore compare the result of these two scenarios in Figure 8. As can be seen, both scenarios provide very similar results, suggesting that the FP calculations can also be used to model the cluster-infall scenario.

4.3. A global model for TDE history

As described in the previous sections, we have followed the evolution of the disruption rates of stars for different types of galaxies and evolutionary/SF-history scenarios. Combining the rates we obtained for each galaxy type with the observational information about the fraction of each morphological galaxy type can provide a general prediction for the TDH of the universe. This analysis is done as follows; for each type of hosted MBH mass we obtain the global TDH by integrating the rates we obtained for the different galaxies and MBH mass, weighted by their relative fraction

$$\Gamma_G = \int_{M_{min}}^{M_{max}} \sum_i \Gamma_{G_i}(m_{BH}) n_{G_i}(m_{BH}) dM_{BH} \quad (7)$$

where Γ_{G_i} is the TDE rate for the i -th galaxy type with an MBH of mass m_{BH} , and $n_{G_i}(m_{BH})$ is its fraction of such galaxies in the local universe. The data for the fraction of each galaxy type is taken from observations (Calvi et al. 2012) and the MBH mass function is based on Kelly and Merloni (2012). Note that in practice we use a sum over the MBH masses for which we have made the full calculation, rather than a continuous mass function. We generally find that the TDE rate dependence on the MBH mass goes approximately as $\Gamma_{TDE}^{avg} = c_1 M_\bullet^{-\gamma_1}$, where $\gamma_1 = 0.44$. We separate the rate dependence results for each galaxy type, and find that the MBH mass goes as $\Gamma_{TDE}^E \sim M_\bullet^{-0.31}$, and $\Gamma_{TDE}^S \sim M_\bullet^{-0.62}$, for elliptical and spiral galaxies respectively. These findings of lower TDE rates obtained for higher mass MBHs are

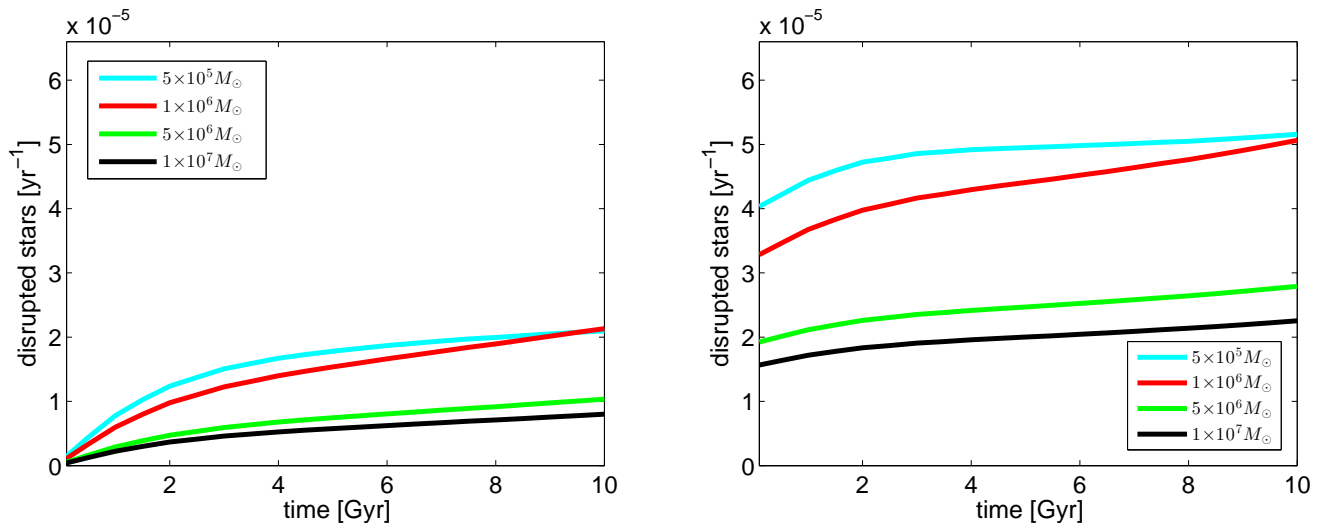


FIG. 7.— Evolution of TDE rates for four models with different masses of MBHs, and a SF history which follows the global universal SF models (Madau and Dickinson 2014) normalized to the NSCs. (the total number of added stars to each model is equal to the total number of stars in models shown in Fig. 1. Left: TDH for NSC evolved from built-up global star formation. Right: TDH for NSC evolved from a primordial cusp with global SF.

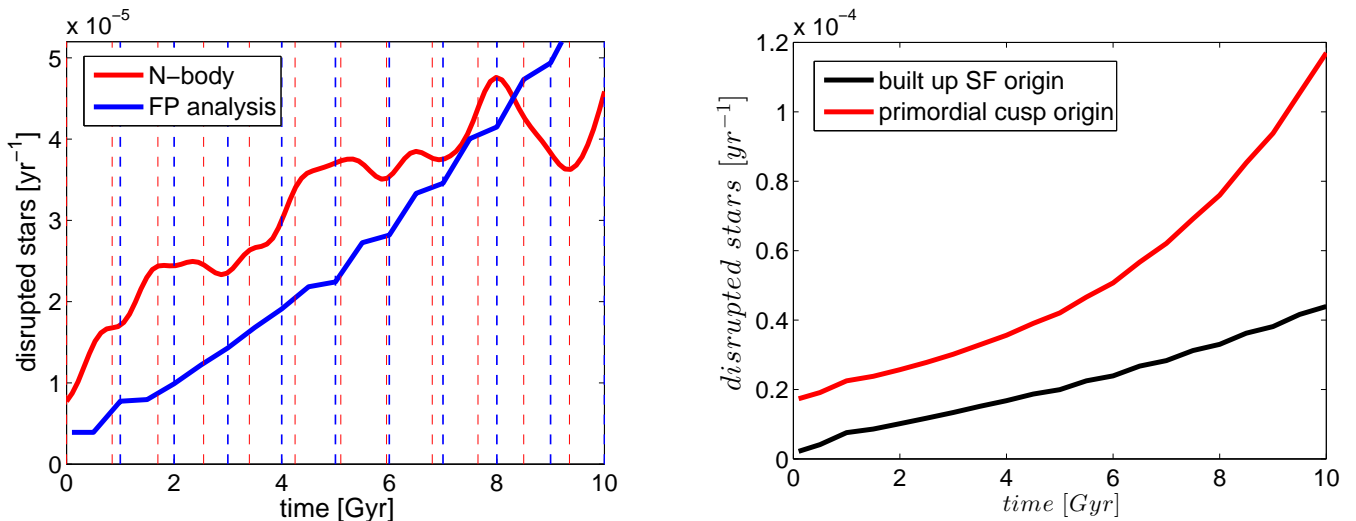


FIG. 8.— Comparison between TDEs history obtained from N-body simulations and FP analysis. TDH for an NSC formed through clusters infall, compared with the TDE history for the FP models with “SF” bursts. The red dashed lines mark the time of the infall (N-body) and the blue dashed lines mark the time of the SF bursts.

not surprising and have already been seen and discussed in depth in other studies. Previous models had not considered continuous SF, however our models for early burst of SF (elliptical galaxies) with no later SF are the most comparable. Indeed in those cases we find consistent results; $\Gamma_{TDE}^E \sim M_{\bullet}^{-0.31}$, where the range of the power law dependence found in previous studies is $0.2 \leq \gamma_1 \leq 0.5$ (e.g. Wang and Merritt 2004; Merritt 2013b; Vasiliev and Merritt 2013; Stone and Metzger 2016).

5. SUMMARY

In our work we provide a first theoretical study of the TDE rate history which considers star-formation and cluster infall scenarios as models for nuclear stellar cluster formation and evolution. We find that in most scenarios the TDE rates grow with time, due to the growth of the NSCs stellar density during their evolution, where the

FIG. 9.— The integrated cosmological history of TDEs rates per galaxy for the built-up and the primordial cusp scenarios for NSC formation and evolution. Note that for these final results we integrated the TDEs rates over MBHs masses between $10^5 M_{\odot}$ and $5 \times 10^7 M_{\odot}$.

TDE rates decrease inversely with the mass of the MBH they host. We explored two different origins of the NSC: pre-existing NSC cusp that forms very early in the galaxy evolution or an NSC that grows more slowly through star formation or cluster infalls. NSCs with primordial cusps have initially larger stellar populations. The overall TDE rates they produce are therefore higher than those calculated for the cases of NSC which are built-up on longer timescales, and they are non-negligible already at early times. Consideration of different types of SF histories, corresponding to elliptical and spiral galaxies, also show a similar trend: the earlier the SF occurs (e.g. in elliptical where most SF is assumed to occur at the first Gyr), the faster the NSC is built, and the faster the TDE rates increase.

We also compared our disruption rates for NSCs with SF which occurs in the inner parsec, and found that in such SF scenarios a the TDE histories show a different

behavior where: during the SF epoch the TDE rates rapidly grow, but then decrease and decay to a much lower level on a timescale of a few Gyrs.

Finally, to complement our main results from the Fokker-Planck models, we also modeled the TDH using data from full N-body simulations of the cluster-infall scenario. We found a good match between these rates and the FP results corresponding to a source term of stars in the NSC outskirts, further confirming the more simplified FP analysis.

Our results are mainly based on simple 1D Fokker-Planck models. Although these appear to be able to well capture the results of N-body simulations (at least for the cluster-infall scenario modeled through N-body simulations), they did not include a detailed galaxy merger history, and more complex non-spherical structures of NSCs. The role of these aspects and their effects on the TDH are not well determined, and should be considered in future work

Future surveys of TDEs (e.g. using the LSST data) would be able to provide not only better estimate of the TDE rates in the local universe, and their dependence on the host galaxy, but also the history of TDEs. As we have shown here, the TDH can provide us with information on the overall evolution of nuclear stellar clusters and the star-formation history and properties in galactic nuclei through the combination of the observational data and the theoretical studies.

We would like to thank Clovis Hopman for the use of the basic components in his FP code for developing the FP code used in our simulations. We would also like to especially thank the anonymous referee for important comments and suggestions that considerably improved the manuscript. We acknowledge support from the Technion Asher Space Research Institute and the I-CORE Program of the Planning and Budgeting Committee and The Israel Science Foundation grant 1829/12.

REFERENCES

- D. Aharon and H. B. Perets. Formation and Evolution of Nuclear Star Clusters with In Situ Star Formation: Nuclear Cores and Age Segregation. *ApJ*, 799:185, February 2015. doi:10.1088/0004-637X/799/2/185.
- F. Antonini, R. Capuzzo-Dolcetta, A. Mastrobuono-Battisti, and D. Merritt. Dissipationless Formation and Evolution of the Milky Way Nuclear Star Cluster. *ApJ*, 750:111, May 2012. doi:10.1088/0004-637X/750/2/111.
- J. N. Bahcall and R. A. Wolf. Star distribution around a massive black hole in a globular cluster. *ApJ*, 209:214–232, October 1976. doi:10.1086/154711.
- J. N. Bahcall and R. A. Wolf. The star distribution around a massive black hole in a globular cluster. II Unequal star masses. *ApJ*, 216:883–907, September 1977. doi:10.1086/155534.
- H. Bartko, F. Martins, T. K. Fritz, R. Genzel, Y. Levin, H. B. Perets, T. Paumard, S. Nayakshin, O. Gerhard, T. Alexander, K. Dodds-Eden, F. Eisenhauer, S. Gillessen, L. Mascetti, T. Ott, G. Perrin, O. Pfuhl, M. J. Reid, D. Rouan, A. Sternberg, and S. Trippe. Evidence for Warped Disks of Young Stars in the Galactic Center. *ApJ*, 697:1741–1763, June 2009. doi:10.1088/0004-637X/697/2/1741.
- M. Brockamp, H. Baumgardt, and P. Kroupa. Tidal disruption rate of stars by supermassive black holes obtained by direct N-body simulations. *MNRAS*, 418:1308–1324, December 2011. doi:10.1111/j.1365-2966.2011.19580.x.
- R. Calvi, B. M. Poggianti, G. Fasano, and B. Vulcani. The distribution of galaxy morphological types and the morphology-mass relation in different environments at low redshift. *MNRAS*, 419:L14–L18, January 2012. doi:10.1111/j.1745-3933.2011.01168.x.
- H. Cohn and R. M. Kulsrud. The stellar distribution around a black hole - Numerical integration of the Fokker-Planck equation. *ApJ*, 226:1087–1108, December 1978. doi:10.1086/156685.
- T. Do, A. M. Ghez, M. R. Morris, J. R. Lu, K. Matthews, S. Yelda, and J. Larkin. High Angular Resolution Integral-Field Spectroscopy of the Galaxy’s Nuclear Cluster: A Missing Stellar Cusp? *ApJ*, 703:1323–1337, October 2009. doi:10.1088/0004-637X/703/2/1323.
- S. Gezari. The tidal disruption of stars by supermassive black holes. *Physics Today*, 67(5):37–42, May 2014. doi:10.1063/PT.3.2382.
- S. Harfst, A. Gualandris, D. Merritt, R. Spurzem, S. Portegies Zwart, and P. Berczik. Performance analysis of direct N-body algorithms on special-purpose supercomputers. *New A*, 12: 357–377, July 2007. doi:10.1016/j.newast.2006.11.003.
- B. C. Kelly and A. Merloni. Mass Functions of Supermassive Black Holes across Cosmic Time. *Advances in Astronomy*, 2012:970858, 2012. doi:10.1155/2012/970858.
- I. Khabibullin and S. Sazonov. Stellar tidal disruption candidates found by cross-correlating the ROSAT Bright Source Catalogue and XMM-Newton observations. *ArXiv e-prints*, July 2014.
- A. P. Lightman and S. L. Shapiro. The distribution and consumption rate of stars around a massive, collapsed object. *ApJ*, 211:244–262, January 1977. doi:10.1086/154925.
- P. Madau and M. Dickinson. Cosmic Star-Formation History. *ARA&A*, 52:415–486, August 2014. doi:10.1146/annurev-astro-081811-125615.
- J. Magorrian and S. Tremaine. Rates of tidal disruption of stars by massive central black holes. *MNRAS*, 309:447–460, October 1999. doi:10.1046/j.1365-8711.1999.02853.x.
- A. Mastrobuono-Battisti, H. B. Perets, and A. Loeb. Effects of Intermediate Mass Black Holes on Nuclear Star Clusters. *ApJ*, 796:40, November 2014. doi:10.1088/0004-637X/796/1/40.
- D. Merritt. Evolution of Nuclear Star Clusters. *ApJ*, 694: 959–970, April 2009. doi:10.1088/0004-637X/694/2/959.
- D. Merritt. Loss-cone dynamics. *Classical and Quantum Gravity*, 30(24):244005, December 2013a. doi:10.1088/0264-9381/30/24/244005.
- D. Merritt. *Dynamics and Evolution of Galactic Nuclei*. July 2013b.
- D. Merritt and L. Ferrarese. The $M_{\text{bulb}}-\sigma$ Relation for Supermassive Black Holes. *ApJ*, 547:140–145, January 2001. doi:10.1086/318372.
- B. W. Murphy, H. N. Cohn, and R. H. Durisen. Dynamical and luminosity evolution of active galactic nuclei - Models with a mass spectrum. *ApJ*, 370:60–77, March 1991. doi:10.1086/169793.
- T. Oka, M. Nagai, K. Kamegai, and K. Tanaka. A New Look at the Galactic Circumnuclear Disk. *ApJ*, 732:120, May 2011. doi:10.1088/0004-637X/732/2/120.
- H. B. Perets and A. Mastrobuono-Battisti. Age and Mass Segregation of Multiple Stellar Populations in Galactic Nuclei and their Observational Signatures. *ApJ*, 784:L44, April 2014. doi:10.1088/2041-8205/784/2/L44.
- H. B. Perets, C. Hopman, and T. Alexander. Massive Perturber-driven Interactions between Stars and a Massive Black Hole. *ApJ*, 656:709–720, February 2007. doi:10.1086/510377.
- M. J. Rees. Tidal disruption of stars by black holes of 10 to the 6th-10 to the 8th solar masses in nearby galaxies. *Nature*, 333: 523–528, June 1988. doi:10.1038/333523a0.
- A. C. Seth, J. J. Dalcanton, P. W. Hodge, and V. P. Debattista. Clues to Nuclear Star Cluster Formation from Edge-on Spirals. *AJ*, 132:2539–2555, December 2006. doi:10.1086/508994.
- N. C. Stone and B. D. Metzger. Rates of stellar tidal disruption as probes of the supermassive black hole mass function. *MNRAS*, 455:859–883, January 2016. doi:10.1093/mnras/stv2281.

S. van Velzen and G. R. Farrar. Measurement of the rate of stellar tidal disruption flares. *ArXiv e-prints*, July 2014.

E. Vasiliev and D. Merritt. The Loss-cone Problem in Axisymmetric Nuclei. *ApJ*, 774:87, September 2013. doi:10.1088/0004-637X/774/1/87.

J. Wang and D. Merritt. Revised Rates of Stellar Disruption in Galactic Nuclei. *ApJ*, 600:149–161, January 2004. doi:10.1086/379767.